Journal of Inorganic and General Chemistry
ZAAC
Zeitschrift für anorganische und allgemeine Chemie
DOI: 10.1002/zaac.201900354
ARTICLE

Influence of CF_3 Substituents on the Spin Crossover Behavior of Iron(II) Coordination Polymers with Schiff Base-like Ligands

Hannah Kurz,[a] Joan Sander,[a] and Birgit Weber*[a]

Dedicated to Professor Manfred Scheer on the Occasion of his 65th Birthday

Abstract. A Schiff base-like ligand bearing CF_3 substituents was synthesized and converted to iron(II) coordination polymers $[\{FeL(L_{ax})\}_n]$ using five different bridging ligands L_{ax}. The structure of the coordination polymers was investigated using powder X-ray diffraction and single-crystal X-ray diffraction in the case of $[\{FeL(bipy)\}_n]$. The later revealed an untypical ABAB pattern of alternating equatorial ligands rotated by 180° with regard to each other along the chain. The temperature-dependent magnetic behavior was investigated with a SQUID magnetometer and the spin states at room temperature were confirmed by ^{57}Fe-Mössbauer spectroscopy. Three out of five coordination polymers show spin crossover behavior in the temperature range between 50 and 400 K with different kind of curve progressions (abrupt, gradual, step-wise). The other two coordination polymers are either fully highspin or fully low spin.

Introduction

Bistable switchable materials are of high interest for applications in the field of molecular sensors.[1,2] For this purpose, a well suited class of compounds are spin crossover (SCO) complexes. These compounds can be switched between the high spin (HS) and the low spin (LS) state by external physical stimuli such as a variation of temperature, pressure, or light irradiation. The SCO leads to discrete changes in the structural, optical, and magnetic properties of the material. Therefore, it can be followed by many complementary methods such as temperature-dependent X-ray diffraction, UV/Vis spectroscopy, or magnetic measurements.[2,3] These changes can be combined with additional properties such as luminescence,[4] phase transitions,[5] or redox-active behavior[6] to receive multifunctional materials. In recent years the nanostructuring or surface functionalization of switchable materials was investigated by many research groups as this is an important step towards possible applications such as molecular sensors.[7]

Mostly, spin crossover research concentrates on octahedral iron(II) complexes due to the drastic magnetic change from the diamagnetic LS ($S = 0$) state to the paramagnetic HS ($S = 2$) state upon SCO. For applications an abrupt SCO around room temperature with a broad hysteresis is desired.[8,9] This demands a high cooperativity between the iron(II) metal centers. The impact of short-range interactions such as hydrogen bonds[10] or π–π stacking[11,12] has been put into evidence for many mononuclear complexes in the last decade. Another approach to receive cooperativity is the introduction of long-range interactions through 1D coordination polymers.[13] In recent years the well-known Jäger Schiff base-like system[14,15] was studied extensively, as the iron(II) complexes often showed SCO behavior both, as mononuclear[16] and dinuclear complexes[17,18] and as 1D coordination polymers[19,20] and ladder-type polymers.[21] Processing of these polymers is often hampered by their low solubility due to strong intermolecular interactions. Introduction of CF_3 substituents has been found to weaken the non-covalent interactions in many cases.[22] Therefore, CF_3 substituents were introduced to our 1D coordination polymers in order to increase their solubility and decrease the influence of short-range interactions. Indeed, in previous work by *Saloutin* et al. on nickel(II) complexes bearing CF_3 substituents no short-range interactions were reported.[23] In addition, the electron withdrawing effect of the CF_3 substituents is expected to alter the ligand field strength of the iron(II) metal center and thus the SCO behavior on the molecular level.

Herein we present five iron(II) coordination polymers with different axial ligands based on Saloutin's previously mentioned Schiff base-like ligand system.[23] One crystal structure of a coordination polymer was obtained and PXRD patterns of all compounds were investigated. Moreover, the magnetic behavior of all coordination polymers was investigated in detail using magnetic susceptibility measurements and Mössbauer spectroscopy.

Results and Discussion

Synthesis

The 1D coordination polymers were synthesized in three steps as shown in the synthetic pathway in Scheme 1. In the

* Prof. Dr. B. Weber
E-Mail: weber@uni-bayreuth.de
[a] Department of Chemistry
University of Bayreuth
Universitätsstraße 30, NWI
95447 Bayreuth, Germany
Supporting information for this article is available on the WWW under **http://dx.doi.org/10.1002/zaac.201900354** or from the author.

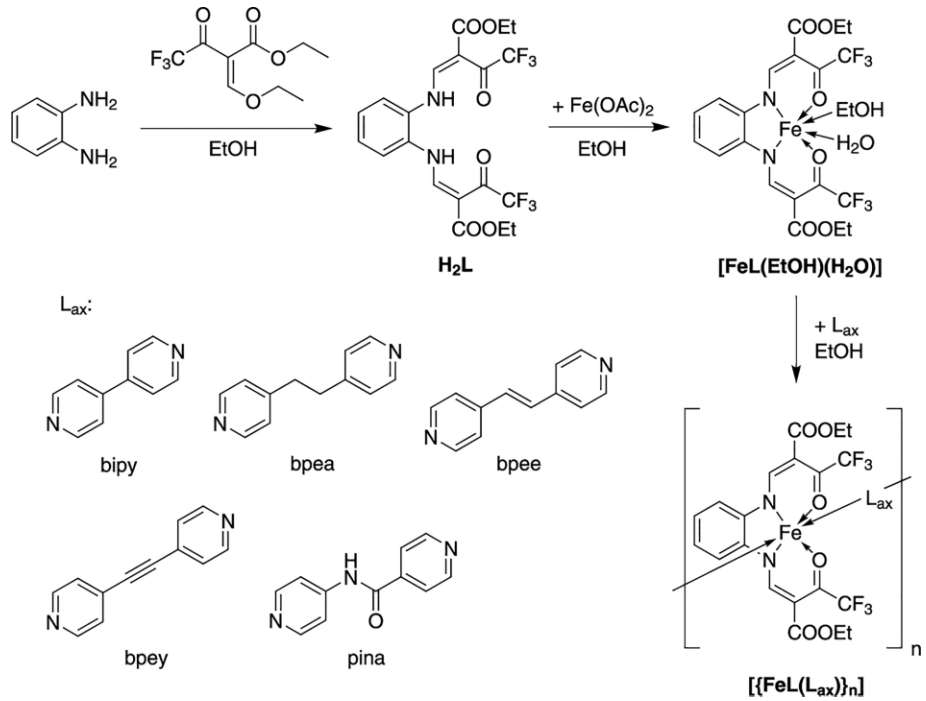

Scheme 1. General pathway for the synthesis of the ligand $\mathbf{H_2L}$, the iron(II) precursor complex **[FeL(EtOH)(H_2O)]**, and the 1D coordination polymers $\mathbf{[\{FeL(L_{ax})\}_n]}$ discussed in this work. The structures of the axial ligands 4,4′-bipyridine (bipy), 1,2-bis(4-pyridyl)ethane (bpea), 1,2-bis(4-pyridyl)ethylene (bpee), 1,2-bis(4-pyridyl)ethyne (bpey), and *N*-(pyrid-4-yl)isonicotinamide (pina) are given.

first step, the Schiff base-like chelate ligand was synthesized in a condensation reaction between *o*-phenylenediamine and the keto-enol ether ethyl-2-(ethoxymethylen)-4,4,4-trifluoro-3-oxobutyrate. The ligand was obtained as a white solid in 93 % yield. The identity and purity was confirmed with ^{1}H NMR and IR spectroscopy, mass spectrometry, and elemental analysis. In the following, the ligand was converted with iron(II) acetate[24] to the iron(II) precursor complex **[FeL(EtOH)(H_2O)]**. The acetate acts as a base in this reaction and deprotonates the ligand. The iron(II) precursor is highly soluble compared to other iron(II) complexes of this general ligand type.[25] In order to obtain **[FeL(EtOH)(H_2O)]** as a solid material, water needs to be added to receive small needles in 73 % yield. The identity and purity of the mononuclear complex was confirmed by IR spectroscopy, mass spectrometry and elemental analysis.

The 1D coordination polymers $\mathbf{[\{FeL(L_{ax})\}_n]}$ were synthesized by ligand exchange with the respective bidentate axial ligand. All coordination polymers precipitated as black solids in yields of 50–87 %. Please note that the yields are lower than other coordination polymers of this general ligand type, indicating a higher solubility. Moreover, all coordination polymers were characterized by IR spectroscopy, mass spectrometry and elemental analysis. According to the elemental analysis no additional solvent is present in the crystal packing of all compounds.

X-ray Diffraction Analysis

Black needle-like crystals suitable for X-ray structure analysis of $\mathbf{[\{FeL(bipy)\}_n]}$ were obtained by a slow diffusion setup of **[FeL(EtOH)(H_2O)]** and 4,4′-bipyridine in ethanol. The crystallographic data were collected at 133 K and are summarized in Table S1 (Supporting Information). The 1D coordination polymer crystallizes as a solvent-free material in the monoclinic space group *C*2/*c*. The asymmetric unit consists of half a molecule. A representation of the structure is shown in Figure 1 (top) and selected bond lengths and angles are summarized in Table 1.

The iron(II) metal center is enclosed in a N_4O_2 coordination sphere, consisting of N_2O_2 of the equatorial ligand and N_2 through the axial bridging ligands. The bond lengths in the equatorial chelate ring are 1.92 Å (Fe–O_{eq}), 1.90 Å (Fe–N_{eq}), and the bond angle of O_{eq}–Fe1–O_{eq} is 88°. The bond length of the metal center to the axial ligand is 1.99 Å (Fe–N_{ax}) with a bond angle of 173° (N_{ax}–Fe–N_{ax}). This bond angle differs slightly from the expected 180° angle of a perfectly octahedral coordination sphere. These values are in the typical range for octahedral iron(II) LS species of this ligand type.[15,26]

Figure 1 (bottom) displays illustrations of the coordination chain. In the polymer chain, each equatorial ligand is twisted by 180° with regard to the next equatorial ligand in the chain. This leads to an ABAB order. Comparison with the crystal structure of a closely related iron(II) coordination polymer $\mathbf{[\{FeL'(bipy)\}_n]}$, that bears CH_3 instead of CF_3 substituents, reveals that the introduction of CF_3 in the equatorial plane induces major structural consequences.[27] Notably an AAAA order has also been reported for all other bipy-bridged coordination polymers with slightly varied equatorial ligands, see $\mathbf{[\{FeL''(bipy)\}_n]}$ at the bottom of Figure 1.[28] The CF_3 groups seem to induce the uncommon twisting.

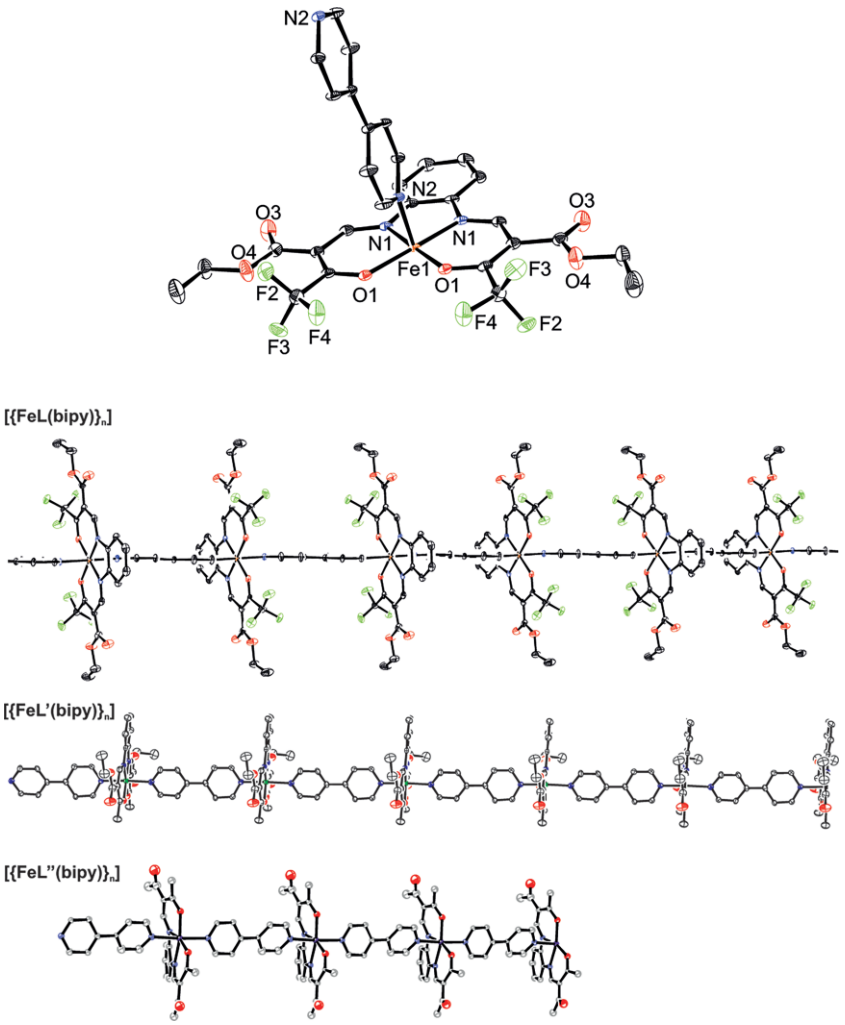

Figure 1. Structure of the propagating unit in **[{FeL(bipy)}$_n$]** (top). Structure of the 1D chain (bottom). For comparison the 1D chains of **[{FeL′(bipy)}$_n$]** with CH_3 instead of CF_3 and **[{FeL′′(bipy)}$_n$]** with a CH_3 group and $COCH_3$ instead of COOEt are given as well. Hydrogen atoms are omitted for clarity. Ellipsoids are drawn at 50 % probability level.

Table 1. Selected bond lengths /Å and angles /° of **[{FeL(bipy)}$_n$]**.

Bond	Bond length	Bonds	Bond angle
Fe1–O1	1.9225(13)	O1–Fe1–O1	87.66(5)
Fe1–N1	1.8951(15)	N2–Fe1–N2	173.07(6)
Fe1–N2	1.9886(15)		

The linear polymer chains are parallel to each other forming a plane as well as the equatorial ligands. These two planes order in a non-orthogonal way with an angle of 84°. The two planes lead to a fence like packing along [010] (see Figure 2). The carbonyl oxygen of the equatorial ligand is connected to the pyridyl ring of a neighboring axial ligand through hydrogen bonds. The two aromatic CH groups (C14–H14 and C15–H15) of the axial ligand bipy act as donor groups and the carbonyl oxygen O2 of the equatorial ligand acts as the acceptor. Details to all observed short range interactions are given in Tables S2 and S3 (Supporting Information). The distance of the fluorine atom F1 and the hydrogen H11 is 2.59 Å with a F1···H11–C11 angle of 126°; the distance of the fluorine atom F3 with the hydrogen atom H12 is 2.60 Å with a F3···H12–C12 angle of 139°. These values might indicate the presence of weak intermolecular C–H···F–C interactions.[29]

Powder diffraction patterns of the iron(II) precursor and all 1D coordination polymers were recorded (see Figure S1, Supporting Information). Firstly, the PXRD patterns confirm a successful and complete conversion to the coordination polymers as characteristic reflexes of the precursor complex are no longer observed. Moreover, the calculated diffraction pattern of **[{FeL(bipy)}$_n$]** based on the single-crystal data is in good agreement to the measured one. This strongly suggests that the molecular structure of the crystal is conserved in the microcrystalline bulk material. The PXRD patterns of all 1D polymers differ strongly, which reflects a quite different molecular packing.

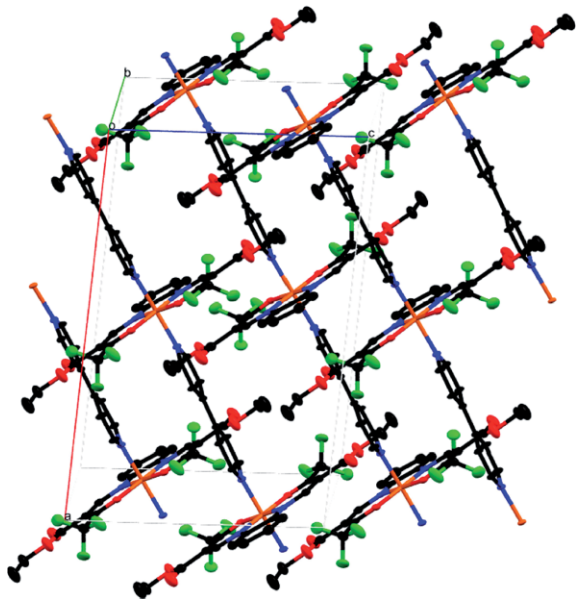

Figure 2. Molecular packing of **[{FeL(bipy)}$_n$]**. Hydrogen atoms are omitted for clarity.

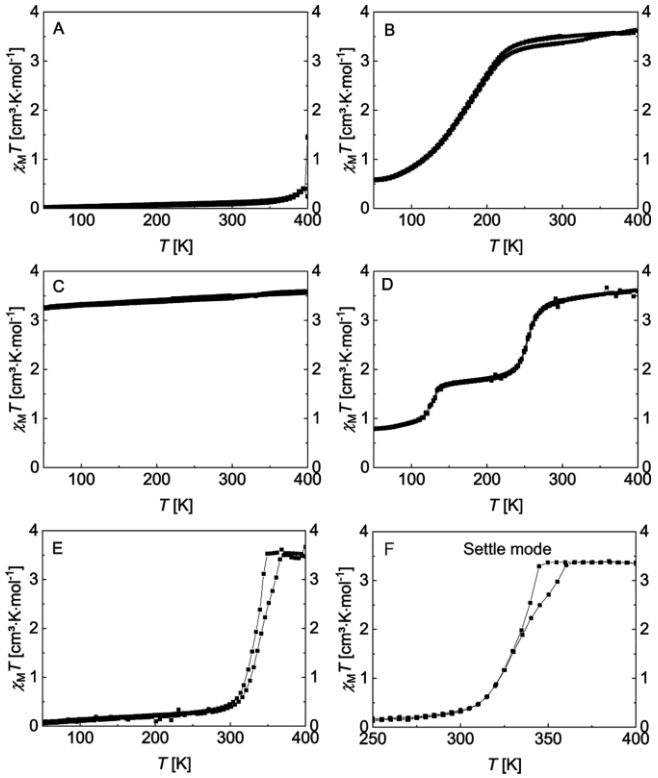

Figure 3. Plots of the $\chi_M T$ product vs. T for the compounds **[{FeL(bipy)}$_n$]** (A), **[{FeL(bpea)}$_n$]** (B), **[{FeL(bpee)}$_n$]** (C), **[{FeL(bpey)}$_n$]** (D), **[{FeL(pina)}$_n$]** (E) measured in the sweep mode (5 K·min^{-1}). Plot of the $\chi_M T$ product vs. T for the compound **[{FeL(pina)}$_n$]** measured in the settle mode in the temperature range 250–400 K (F).

Magnetism

Temperature-dependent magnetic susceptibility measurements were performed for all fine crystalline 1D coordination polymers using a SQUID magnetometer. Unfortunately, single crystals of **[{FeL(bipy)}$_n$]** could not be investigated as not enough crystals could be collected. Nevertheless, the PXRD measurements show a high similarity between bulk and crystal. The $\chi_M T$ product was plotted against T for all five samples in the temperature range 50–400 K and is shown in Figure 3. An overview of the characteristic magnetic data of the polymers is given in Table 2. Theoretically, at room temperature a $\chi_M T$ value of nearly 0 cm^3 K mol^{-1} is expected for iron(II) in the diamagnetic LS state. Whereas, a $\chi_M T$ value of approximately 3.5 cm^3·K·mol^{-1} is expected for iron(II) in the paramagnetic HS state.[12,19]

Intriguingly, the 1D polymers **[{FeL(L$_{ax}$)}$_n$]** cover the whole phenomenological range of SCO materials when the bridging ligand **L$_{ax}$** is varied; showing the two extremes HS and LS as well as different kind of SCO behavior (abrupt, gradual, and step-wise). The magnetic measurement of **[{FeL(bipy)}$_n$]** shows a diamagnetic behavior in the temperature range of 50–360 K. Upon heating to 400 K the $\chi_M T$ value begins to increase, indicating that a SCO takes place above 400 K. The compound **[{FeL(bpea)}$_n$]** shows an incomplete gradual spin transition, which takes place between 50 and 260 K with a $T_{1/2}$ of 181 K. The compound **[{FeL(bpee)}$_n$]** is in the HS state over the whole temperature range. The $\chi_M T$ value remains at approximately 3.5 cm^3·K·mol^{-1}, which is typical for iron(II) in the HS state. The magnetic measurements of **[{FeL(bpey)}$_n$]** show an incomplete two-step spin crossover. Upon cooling the $\chi_M T$ product decreases around 254 K from the room temperature value of 3.4 cm^3 K mol^{-1} to 1.8 cm^3·K·mol^{-1} at 200 K. Around 129 K the second step takes

Table 2. Overview of the SCO behavior, characteristic $\chi_M T$ /cm^3·K·mol^{-1} values (50 K, 300 K, and 400 K), and $T_{1/2}$ /K of the 1D coordination polymers.

Compound	Description of SCO behavior	$\chi_M T$ (50 K)	$\chi_M T$ (300 K)	$\chi_M T$ (400 K)	$T_{1/2}$
[{FeL(bipy)}$_n$]	LS; SCO above 400 K	0.02	0.09	1.45	–
[{FeL(bpea)}$_n$]	Incomplete gradual SCO	0.57	3.50	3.62	181
[{FeL(bpee)}$_n$]	HS	3.26	3.49	3.57	–
[{FeL(bpey)}$_n$]	Incomplete two-step SCO	0.79	3.38	3.59	129 254
[{FeL(pina)}$_n$] [a]	Abrupt SCO with hysteresis	0.06	0.42	3.47	↑ 341 ↓ 334
[{FeL(pina)}$_n$] [b]	Two-step SCO with hysteresis	–	0.32	3.37	↑ 342 ↓ 355

a) Measured in the sweep mode. b) Measured in the settle mode in the temperature range from 250–400 K.

place from 1.7 cm^3·K·mol^{-1} at 160 K to 0.8 cm^3·K·mol^{-1} at 100 K. Finally, the sample **[{FeL(pina)}$_n$]** shows an abrupt SCO above room temperature. At room temperature a $\chi_M T$ product of 0.1 cm^3·K·mol^{-1} is observed, which can be assigned to the LS state. An abrupt SCO is observed around 338 K leading to a $\chi_M T$ product of 3.4 cm^3·K·mol^{-1} at 370 K, which can be assigned to iron(II) in the HS state. In the sweep mode (5 K·min^{-1}) a small hysteresis with a width of 7 K is observed as shown in Figure 3E. A small hysteresis like this might be based on kinetic effects. For this reason, the magnetic measurement is repeated in the settle mode (Figure 3F). This demonstrates that on one hand the previously observed hysteresis is indeed based on a kinetic effect. On the other hand, a two-step SCO is observed in the heating mode, leading to a small hysteresis of 12 K with $\downarrow T_{1/2}$ of 355 K and $\uparrow T_{1/2}$ of 342 K.

The temperature-dependent magnetic behavior of **[{FeL(L$_{ax}$)}$_n$]** can be compared to the otherwise identical set of 1D coordination polymers **[{FeL′(L$_{ax}$)}$_n$]** bearing CH_3 substituents instead of CF_3. The behavior of the coordination polymer with bipy differs significantly, as HS over the whole temperature region was reported for the CH_3 polymer. The previously discussed divergence in the structural pattern is reflected by the strongly contrasting magnetic behavior. These drastic differences in the magnetic behavior do not persist for all CH_3/CF_3 couples. For example, the effect of CH_3/CF_3 substituents on the magnetic behavior is only marginal in the polymers with bpea and bpee. Both bpea polymers show a gradual incomplete SCO below room temperature.[27] Irrespective of substitution the polymers with bpee as the bridging ligand are HS over the whole temperature range.[18] Similarity among the CH_3/CF_3 couples was observed as well for the coordination polymers with bpey as axial ligand. Both coordination polymers show a stepwise SCO below room temperature. In case of CH_3 as substituent even a three-step SCO was obtained.[30] Finally, the polymer with pina as axial ligand shows an abrupt SCO above room temperature, whereas the CH_3 analog is HS over the whole temperature range.[31] Indeed, slightly different 1D coordination polymers with pina showed an abrupt SCO with a broad hysteresis.[8]

In summary, the magnetic behavior of the 1D coordination polymers bearing a CF_3 substituent do not differ significantly from the coordination polymer with a CH_3 substituent in three out of five cases. In the remaining two cases with bipy and bpea as axial ligands a strong difference in the magnetic behavior was observed. A correlation of the SCO behavior with the nature of the linker or substituents of the equatorial ligand is not evident. Nevertheless, it can be noted that the weakening effect of the electron withdrawing CF_3 substituents on the ligand field strength is rather small. It does not have a strong effect on the magnetic behavior as the SCO behavior is not varied systematically to a higher or lower $T_{1/2}$. The differences in the magnetic behavior seem to be rather based on the effects of the CF_3 substituents on the molecular packing.

^{57}Fe Mössbauer Spectroscopy

Room temperature Mössbauer spectroscopy was performed for all 1D coordination polymers to confirm the spin state assignment and to prove the presence of just one iron(II) site in each compound. The Mössbauer spectra of all samples are given in Figure 4 and the fit parameters summarized in Table 3. **[{FeL(bipy)}$_n$]** and **[{FeL(pina)}$_n$]** show one doublet with a chemical shift of δ = 0.30–0.35 mm·s^{-1} and a quadrupole splitting of ΔE_Q = 1.2 mm·s^{-1}, which is typical for iron(II) in the LS state for such octahedral complexes.[19] In full agreement with the conclusions from the SQUID measurements,

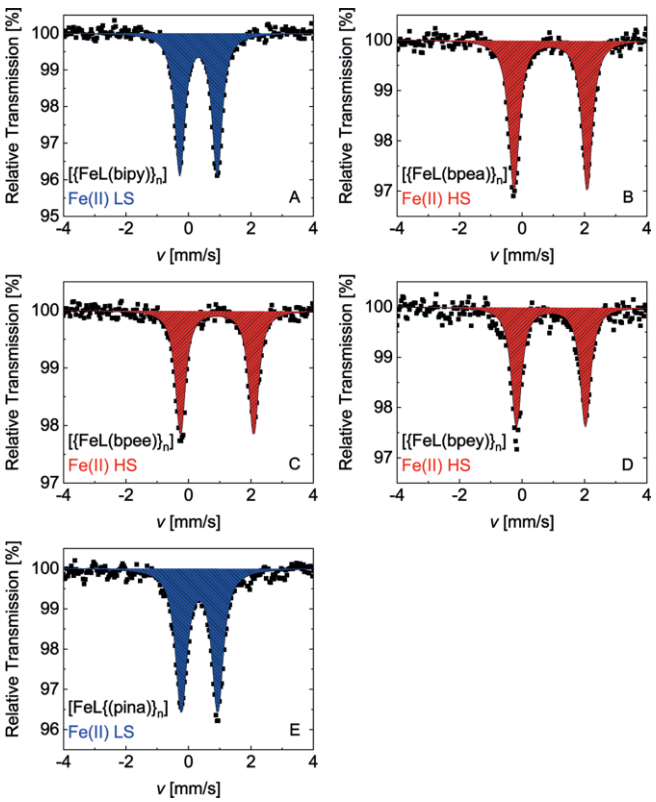

Figure 4. Room temperature ^{57}Fe Mössbauer spectra of **[{FeL(bipy)}$_n$]** (A), **[{FeL(bpea)}$_n$]** (B), **[{FeL(bpee)}$_n$]** (C), **[{FeL(bpey)}$_n$]** (D), **[{FeL(pina)}$_n$]** (E). The area of the iron(II) LS doublet has a blue color, the area of the iron(II) HS doublet has a red color.

Table 3. ^{57}Fe Mössbauer data of the 1D coordination polymers.

Compound	Site	δ /mm·s^{-1}	ΔE_Q /mm·s^{-1}	$\Gamma/2$ /mm·s^{-1}
[{FeL(bipy)}$_n$]	Fe^{II} LS	0.321(5)	1.198(10)	0.186(7)
[{FeL(bpea)}$_n$]	Fe^{II} HS	0.915(6)	2.342(12)	0.191(9)
[{FeL(bpee)}$_n$]	Fe^{II} HS	0.916(7)	2.345(14)	0.185(11)
[{FeL(bpey)}$_n$]	Fe^{II} HS	0.926(10)	2.208(2)	0.190(16)
[{FeL(pina)}$_n$]	Fe^{II} LS	0.352(7)	1.164(14)	0.212(10)

[{FeL(bpea)}$_n$], **[{FeL(bpee)}$_n$]**, and **[{FeL(bpey)}$_n$]** present one broad doublet with a chemical shift of δ = 0.9 mm·s^{-1} and a quadrupole splitting of ΔE_Q = 2.2–2.3 mm·s^{-1}. These values are typical for octahedral coordinated iron(II) in the HS state.[19] The values correspond nicely to the magnetic measurements recorded with the SQUID magnetometer. Moreover, the Mössbauer measurements confirm that only one iron(II) species is present in each sample, ruling out the presence of iron impurities or oxidation of the samples.

Conclusions

An equatorial Schiff base-like ligand bearing electron withdrawing CF_3 substituents was synthesized and successfully converted into five new 1D iron(II) coordination polymers with different axial ligands. The crystal structure of the 1D coordination polymer **[{FeL(bipy)}$_n$]** revealed the twisting of the equatorial ligands by 180° to the next equatorial ligand in line, leading to an ABAB alternating pattern. This uncommon twisting was not observed for a similar iron(II) 1D coordination polymer bearing CH_3 instead of CF_3. The magnetic properties were investigated with a SQUID magnetometer and Mössbauer spectra were recorded of all compounds. Two major conclusions can be drawn: Firstly, the SCO behavior differs significantly among the 1D coordination polymers **[{FeL(L$_{ax}$)}$_n$]**. The complete phenomenological range of SCO is covered, allowing no obvious correlation with the nature of the ligand. Three out of five coordination polymers feature thermal SCO. Especially, **[{FeL(pina)}$_n$]** could be interesting for further applications due to the abrupt SCO above room temperature. Secondly, the comparison of the temperature-dependent magnetic behavior with the respective CH_3 analogs **[{FeL′(L$_{ax}$)}$_n$]** with the same axial ligand show in most cases very similar behavior. This and the high variety of SCO behavior indicates that the CF_3 substituents do not have a strong effect on the ligand field strength of the iron(II) metal center. The differences in the SCO behavior seem to be based on differences in the molecular packing induced by the CF_3 substituents. So far, the influence of the CF_3 substituents on possible short range interactions could not be investigated for all complexes as up to now no more crystals could be obtained. However, the CF_3 substituents seem to have a lowering impact on short range interactions leading to a higher solubility. In further work the keto-enol ether bearing CF_3 will be used to increase the solubility of poorly soluble heteroaromatic ligands and their respective complexes.

Experimental Section

Synthesis: Iron(II) acetate,[24] 1,2-bis(4-pyridyl)ethyne,[30] and *N*-(pyrid-4-yl)isonicotinamide[8] were synthesized as described in literature. Ethyl-2-(ethoxymethylen)-4,4,4-trifluoro-3-oxobutyrat (>96 %, TCI), *o*-phenylenediamine (98 %, Acros Organics), 4,4′-bipyridine (98 %, Alfa Aesar), 1,2-bis(4-pyridyl)ethane (97 %, Acros Organics), and 1,2-bis(4-pyridyl)ethylene (97 %, Sigma Aldrich) were used without further purification. Ethanol was of analytical grade and used without further purification. All air sensitive syntheses were carried out under argon 5.0 using Schlenk tube techniques. The solvents were flushed for 30 min with Argon 5.0. NMR spectra were recorded with a 500 MHz Avance III HD NMR spectrometer from Bruker. CHN analyses were performed with an Unicube from Elementar Analysen Systeme. The samples were prepared in a tin boat and sulfanilamide was used as standard. Mass spectra were recorded with a Finnigan MAT 8500 with a data system MASPEC II.

X-ray Structure Analysis: The X-ray analysis of **[{FeL(bipy)}$_n$]** was performed with a Stoe StadiVari diffractometer using graphite-monochromated Mo-K_α radiation. The data were corrected for Lorentz and polarization effects. The structures were solved by direct methods (SIR-97)[32] and refined by full-matrix least-square techniques against Fo2–Fc2 (SHELXL-97).[33] All hydrogen atoms were calculated in idealized positions with fixed displacement parameters. ORTEP-III[34] was used for the structure representation, Mercury-3.10[35] to illustrate molecule packing.

X-ray Powder Diffraction: Powder diffractograms were recorded with a STOE StadiP diffractometer using Cu-K_α1 radiation with a Ge monochromator, and a Mythen 1 K Stripdetector in transmission geometry.

Magnetic Measurements: Magnetic measurements were carried out using a SQUID MPMS-XL5 magnetometer from Quantum Design. A magnetic field of 5000 Oe was applied and the samples were measured in the range from 400 to 50 K in sweep mode (5 K·min^{-1}). The samples were placed in a gelatin capsule held in a plastic straw. The raw data was corrected for the diamagnetism of the sample holder and the organic ligand using tabulated Pascal's constants**.** $K_3[Fe(CN)_6]$ was used as a paramagnetic standard for the magnetic measurements of [FeL(pina)]$_n$ to prevent a loss of the signal due to the abrupt spin crossover above room temperature.

^{57}Mössbauer Spectroscopy: ^{57}Fe Mössbauer spectra were recorded in transmission geometry in a constant-acceleration mode using a conventional Mössbauer spectrometer equipped with a 50 mCi^{57}Co(Rh) source. The samples were prepared in an argon atmosphere. The spectra were fitted using Recoil 1.05 Mössbauer Analysis Software.[36] The isomer shifts were reported with respect to α-Fe as a reference at room temperature.

H_2L: *o*-Phenylenediamine (1.00 g, 9.25 mmol, 1 equiv.) and ethyl-2-(ethoxymethylene)-4,4,4-trifluoro-3-oxobutyrat (6.66 g, 27.74 mmol, 3 equiv.) were dissolved in 100 mL EtOH. The yellow solution was heated to 70 °C for 2 h. After cooling in the fridge overnight, the white precipitate was filtered off and washed with EtOH. Yield: 4.27 g (93 %). **^{1}H NMR** (500 MHz, $CDCl_3$, 25 °C): δ = 12.14 [d, ^3J(NH–NCH) = 13.0 Hz, 2 H, –NH]; 8.51 [d, ^3J(NH–NCH) = 13.0 Hz, 2 H, NC–H]; 7.44 (m, 2 H, Ar–H); 7.40 (m, 2 H, Ar–H); 4.31 [q, ^3J(CH2–CH3) = 7.0 Hz, 4 H, –CH2]; 1.34 [t, ^3J(CH2–CH3) = 7.0 Hz, 6 H, –CH3] ppm. **MS** (DEI-(+), 70 eV): *m*/*z* = 496 (M+, 33 %). $C_{20}H_{18}F_6N_2O_6$ (496.36 g·mol^{-1}): C 48.22 (calcd. 48.40); H 3.37 (3.66); N 5.89 (5.64) %. **IR**: $\tilde{\nu}$ = 3456 (b, N–H), 1724 (s, C=O), 1698 (s, C=O), 1153 (s, C–F) cm^{-1}.

[FeL(EtOH)(H_2O)]: H_2L (2.00 g, 4.03 mmol, 1 equiv.) and iron(II) acetate (0.91 g, 5.24 mmol, 1.3 equiv.) were dissolved in 90 mL degassed EtOH. The dark brown solution was heated to reflux for 1 h. Upon cooling 70 mL degassed water was added dropwise. After storing the suspension at room temperature overnight, the red-brown precipitate was filtered off and washed three times with 5 mL of a EtOH/H_2O (1:1) mixture. Yield: 1.81 g (73 %). **MS** (DEI-(+), 70 eV): *m*/*z* = 550 (M+-EtOH-H_2O, 100 %). $C_{22}H_{24}F_6FeN_2O_8$ (614.28 g·mol^{-1}): C

43.01 (calcd. 43.02); H 3.56 (3.94); N 4.64 (4.56)%. **IR**: $\tilde{\nu}$ = 3456 (b, O–H), 1678 (s, C=O), 1150 (s, C–F) cm^{-1}.

[{FeL(bipy)}$_n$]: [FeL(EtOH)(H_2O)] (0.16 g, 0.26 mmol, 1 equiv.) and 4,4′-bipyridine (0.39 g, 2.47 mmol, 9.5 equiv.) were dissolved in 12 mL degassed EtOH. The dark brown solution was heated to reflux for 2 h. After storing the solution at room temperature overnight, a black precipitate was filtered off and washed two times with 2 mL degassed EtOH. Yield: 0.16 g (87 %). **MS** (DEI-(+), 70 eV): *m*/*z* = 156 (bipy, 100 %), 550 (M+-bipy, 29 %). $C_{30}H_{24}F_6FeN_4O_6$ (706.38 g·mol^{-1}): C 51.06 (calcd. 51.01); H 3.50 (3.42); N 8.03 (7.93) %. **IR**: $\tilde{\nu}$ = 1679 (s, C=O), 1142 (s, C–F) cm^{-1}.

[{FeL(bpea)}$_n$]: [FeL(EtOH)(H_2O)] (0.25 g, 0.41 mmol, 1 equiv.) and 1,2-bis(4-pyridyl)ethane (0.72 g, 3.87 mmol, 9.5 equiv.) were dissolved in 20 mL degassed EtOH. The dark brown solution was heated to reflux for 2 h. After storing the solution at room temperature overnight, a black precipitate was filtered off and washed two times with 2 mL degassed EtOH. Yield: 0.17 g (56 %). **MS** (DEI-(+), 70 eV): *m*/*z* = 184 (bpea, 100 %), 550 (M+–bpea, 27 %). $C_{32}H_{28}F_6FeN_4O_6$ (734.43 g·mol^{-1}): C 52.19 (calcd. 52.33); H 3.73 (3.84); N 7.70 (7.63) %. **IR**: $\tilde{\nu}$ = 1709 (s, C=O), 1146 (s, C–F) cm^{-1}.

[{FeL(bpee)}$_n$]: [FeL(EtOH)(H_2O)] (0.14 g, 0.23 mmol, 1 equiv.) and 1,2-bis(4-pyridyl)ethylene (0.40 g, 2.18 mmol, 9.5 equiv.) were dissolved in 10 mL degassed EtOH. The dark brown solution was heated to reflux for 2 h. After storing the solution at room temperature overnight, a black precipitate was filtered off and washed two times with 2 mL degassed EtOH. Yield: 0.13 g (77 %). **MS** (DEI-(+), 70 eV): *m*/*z* = 181 (bpee, 100 %), 550 (M+-bpee, 68 %). $C_{32}H_{26}F_6FeN_4O_6$ (732.42 g·mol^{-1}): C 52.56 (calcd. 52.48); H 3.49 (3.58); N 7.64 (7.65) %. **IR**: $\tilde{\nu}$ = 1688 (s, C=O), 1142 (s, C–F) cm^{-1}.

[{FeL(bpey)}$_n$]: [FeL(EtOH)(H_2O)] (0.13 g, 0.21 mmol, 1 equiv.) and 1,2-bis(4-pyridyl)ethyne (0.36 g, 2.01 mmol, 9.5 equiv.) were dissolved in 10 mL degassed EtOH. The dark brown solution was heated to reflux for 2 h. After storing the solution at room temperature overnight, a black precipitate was filtered off and washed two times with 2 mL degassed EtOH. Yield: 0.13 g (85 %). **MS** (DEI-(+), 70 eV): *m*/*z* = 180 (bpey, 28 %), 550 (M+-bpey, 100 %). $C_{32}H_{24}F_6FeN_4O_6$ (730.40 g·mol^{-1}): C 52.51 (calcd. 52.62); H 3.14 (3.31); N 7.62 (7.67) %. **IR**: $\tilde{\nu}$ = 1713 (s, C=O), 1148 (s, C–F) cm^{-1}.

[{FeL(pina)}$_n$]: [FeL(EtOH)(H_2O)] (0.15 g, 0.24 mmol, 1 equiv.) and *N*-(4-*p*yridyl)isonicotinamide (0.47 g, 2.34 mmol, 9.5 equiv.) were dissolved in 13 mL degassed EtOH. The dark red solution was heated to reflux for 2 h. After storing the solution at room temperature overnight, a brown precipitate was filtered off and washed with 2 mL degassed EtOH. Yield: 0.09 g (50 %). **MS** (DEI-(+), 70 eV): *m*/*z* = 199 (pina, 97 %), 550 (M+-pina, 97 %). $C_{31}H_{25}F_6FeN_5O_7$ (749.40 g·mol^{-1}): C 49.63 (calcd. 49.68); H 3.19 (3.36); N 9.33 (9.35)%. **IR**: $\tilde{\nu}$ = 1681 (s, C=O), 1139 (s, C–F) cm^{-1}.

Supporting Information (see footnote on the first page of this article): In the Supporting Information, the PXRD patterns of all iron complexes and coordination polymers are given. In addition, the crystallographic data are summarized.

Acknowledgements

Financial supports from the Fonds der Chemischen Industrie (Kekulé-Stipendium), the BayNAT program, ENB Elite Network of Bavaria and the University of Bayreuth are gratefully acknowledged. We thank *Dr. Ulrike Lacher* for the measurement of the mass spectra and *Florian Puchtler* for the measurement of the PXRD patterns. Open access funding enabled and organized by Projekt DEAL.

Keywords: Schiff base; Iron; Spin crossover; Magnetic properties

References

[1] a) E. Coronado, *Nature Rev. Mater.* **2019**, *24*, 834; b) Z.-P. Ni, J.-L. Liu, M. N. Hoque, W. Liu, J.-Y. Li, Y.-C. Chen, M.-L. Tong, *Coord. Chem. Rev.* **2017**, *335*, 28–43; c) K. Senthil Kumar, M. Ruben, *Coord. Chem. Rev.* **2017**, *346*, 176–205; d) S. Brooker, *Chem. Soc. Rev.* **2015**, *44*, 2880–2892; e) A. B. Gaspar, M. Seredyuk, *Coord. Chem. Rev.* **2014**, *268*, 41–58; f) P. Gütlich, *Eur. J. Inorg. Chem.* **2013**, *2013*, 581–591; g) P. Gütlich, A. B. Gaspar, Y. Garcia, *Beilstein J. Org. Chem.* **2013**, *9*, 342–391.

[2] M. A. Halcrow (Ed.) *Spin-Crossover Materials*, John Wiley & Sons Ltd, Chichester **2013**.

[3] a) P. Gütlich, H. A. Goodwin (Eds.) *Topics in Current Chemistry*, *233–235*, Springer Berlin / Heidelberg **2004**; b) B. Sieklucka, D. Pinkowicz (Eds.) *Molecular Magnetic Materials*, Wiley-VCH Verlag GmbH & Co. KGaA, Weinheim, Germany **2017**.

[4] a) C. Lochenie, K. Schötz, F. Panzer, H. Kurz, B. Maier, F. Puchtler, S. Agarwal, A. Köhler, B. Weber, *J. Am. Chem. Soc.* **2018**, *140*, 700–709; b) B. Benaicha, K. van Do, A. Yangui, N. Pittala, A. Lusson, M. Sy, G. Bouchez, H. Fourati, C. J. Gómez-García, S. Triki et al., *Chem. Sci.* **2019**, *10*, 6791–6798; c) J. M. Herrera, S. Titos-Padilla, Pope, Simon J. A., I. Berlanga, F. Zamora, J. J. Delgado, K. V. Kamenev, X. Wang, A. Prescimone, E. K. Brechin et al., *J. Mater. Chem. C* **2015**, *3*, 7819–7829; d) C.-F. Wang, R.-F. Li, X.-Y. Chen, R.-J. Wei, L.-S. Zheng, J. Tao, *Angew. Chem. Int. Ed.* **2015**, *54*, 1574–1577; e) H. J. Shepherd, C. M. Quintero, G. Molnár, L. Salmon, A. Bousseksou, in: *Spin-Crossover Materials* (Ed.: M. A. Halcrow), John Wiley & Sons Ltd, Chichester **2013**, 347–373.

[5] a) J. Weihermüller, S. Schlamp, W. Milius, F. Puchtler, J. Breu, P. Ramming, S. Hüttner, S. Agarwal, C. Göbel, M. Hund et al., *J. Mater. Chem. C* **2019**, *7*, 1151–1163; b) T. Romero-Morcillo, M. Seredyuk, M. C. Munoz, J. A. Real, *Angew. Chem. Int. Ed.* **2015**, *54*, 14777–14781; c) C. Gandolfi, G. G. Morgan, M. Albrecht, *Dalton Trans.* **2012**, *41*, 3726–3730.

[6] a) S. Dorbes, L. Valade, J. A. Real, C. Faulmann, *Chem. Commun.* **2005**, 69–71; b) C. Faulmann, K. Jacob, S. Dorbes, S. Lampert, I. Malfant, M.-L. Doublet, L. Valade, J. A. Real, *Inorg. Chem.* **2007**, *46*, 8548–8559; c) M. Nihei, N. Takahashi, H. Nishikawa, H. Oshio, *Dalton Trans.* **2011**, *40*, 2154–2156.

[7] a) D. J. Harding, in: *Advanced Nanomaterials* (Eds.: E. Rentschler, N. Domracheva, M. Caporali), Elsevier, (S. l.) **2018**, 401–426; b) L. Salmon, L. Catala, *C. R. Chim.* **2018**, *21*, 1230–1269; c) B. Weber, *Chem. Eur. J.* **2017**, *23*, 18093–18100; d) H. J. Shepherd, G. Molnár, W. Nicolazzi, L. Salmon, A. Bousseksou, *Eur. J. Inorg. Chem.* **2013**, *2013*, 653–661; e) P. N. Martinho, C. Rajnak, M. Ruben, in: *Spin-Crossover Materials* (Ed.: M. A. Halcrow), John Wiley & Sons Ltd, Chichester **2013**, 375–404; f) C. M. Quintero, G. Félix, I. Suleimanov, J. Sánchez Costa, G. Molnár, L. Salmon, W. Nicolazzi, A. Bousseksou, *Beilstein J. Nanotechnol.* **2014**, *5*, 2230–2239; g) O. Klimm, C. Gobel, S. Rosenfeldt, F. Puchtler, N. Miyajima, K. Marquardt, M. Drechsler, J. Breu, S. Forster, B. Weber, *Nanoscale* **2016**, *8*, 19058–19065; h) C. Göbel, O. Klimm, F. Puchtler, S. Rosenfeldt, S. Förster, B. Weber, *Beilstein J. Nanotechnol.* **2017**, *8*, 1318–1327.

[8] C. Lochenie, W. Bauer, A. P. Railliet, S. Schlamp, Y. Garcia, B. Weber, *Inorg Chem.* **2014**, *53*, 11563–11572.

[9] a) I. A. Gural'skiy, B. O. Golub, S. I. Shylin, V. Ksenofontov, H. J. Shepherd, P. R. Raithby, W. Tremel, I. O. Fritsky, *Eur. J.*

Inorg. Chem. **2016**, *2016*, 3191–3195; b) M. A. Halcrow, *Chem. Lett.* **2014**, *43*, 1178–1188.
[10] a) B. Weber, W. Bauer, T. Pfaffeneder, M. M. Dîrtu, A. D. Naik, A. Rotaru, Y. Garcia, *Eur. J. Inorg. Chem.* **2011**, *2011*, 3193–3206; b) M. M. Dirtu, C. Neuhausen, A. D. Naik, A. Rotaru, L. Spinu, Y. Garcia, *Inorg. Chem.* **2010**, *49*, 5723–5736; c) E. Coronado, M. C. Gimenez-Lopez, C. Gimenez-Saiz, F. M. Romero, *CrystEngComm* **2009**, *11*, 2198–2203.
[11] a) J.-F. Létard, P. Guionneau, E. Codjovi, O. Lavastre, G. Bravic, D. Chasseau, O. Kahn, *J. Am. Chem. Soc.* **1997**, *119*, 10861–10862; b) Z. J. Zhong, J.-Q. Tao, Z. Yu, C.-Y. Dun, Y.-J. Liu, X.-Z. You, *J. Chem. Soc., Dalton Trans.* **1998**, 327–328.
[12] C. Lochenie, A. Gebauer, O. Klimm, F. Puchtler, B. Weber, *New J. Chem.* **2016**, *40*, 4687–4695.
[13] a) J. Krober, E. Codjovi, O. Kahn, F. Groliere, C. Jay, *J. Am. Chem. Soc.* **1993**, *115*, 9810–9811; b) V. Niel, J. M. Martinez-Agudo, M. C. Muñoz, A. B. Gaspar, J. A. Real, *Inorg. Chem.* **2001**, *40*, 3838–3839.
[14] K. Senthil Kumar, Y. Bayeh, T. Gebretsadik, F. Elemo, M. Gebrezgiabher, M. Thomas, M. Ruben, *Dalton Trans.* **2019**, *48*, 15321–15337.
[15] B. Weber, E.-G. Jäger, *Eur. J. Inorg. Chem.* **2009**, 465–477.
[16] a) C. Lochenie, J. Heinz, W. Milius, B. Weber, *Dalton Trans.* **2015**, *44*, 18065–18077; b) B. Weber, E. S. Kaps, C. Desplanches, J.-F. Létard, K. Achterhold, F. G. Parak, *Eur. J. Inorg. Chem.* **2008**, 4891–4898; c) B. Weber, E. Kaps, J. Obel, W. Bauer, *Z. Anorg. Allg. Chem.* **2008**, *634*, 1421–1426.
[17] B. Weber, E. Kaps, *Heteroat. Chem.* **2005**, *16*, 391–397.
[18] W. Bauer, B. Weber, *Inorg. Chim. Acta* **2009**, *362*, 2341–2346.
[19] W. Bauer, C. Lochenie, B. Weber, *Dalton Trans.* **2014**, *43*, 1990–1999.
[20] a) T. M. Pfaffeneder, S. Thallmair, W. Bauer, B. Weber, *New J. Chem.* **2011**, *35*, 691–700; b) W. Bauer, T. Pfaffeneder, K. Achterhold, B. Weber, *Eur. J. Inorg. Chem.* **2011**, 3183–3192.
[21] W. Bauer, S. Schlamp, B. Weber, *Chem. Commun.* **2012**, *48*, 10222.
[22] R. Berger, G. Resnati, P. Metrangolo, E. Weber, J. Hulliger, *Chem. Soc. Rev.* **2011**, *40*, 3496–3508.
[23] Y. S. Kudyakova, M. V. Goryaeva, Y. V. Burgart, P. A. Slepukhin, V. I. Saloutin, *Russ. Chem. Bull.* **2010**, *119*, 1582–1593.
[24] B. Weber, R. Betz, W. Bauer, S. Schlamp, *Z. Anorg. Allg. Chem.* **2011**, *637*, 102–107.
[25] a) B. Weber, E.-G. Jäger, *Z. Anorg. Allg. Chem.* **2009**, *635*, 130–133; b) W. Bauer, T. Ossiander, B. Weber, *Z. Naturforsch. B* **2010**, 323–328.
[26] B. Weber, *Coord. Chem. Rev.* **2009**, *253*, 2432–2449.
[27] W. Bauer, W. Scherer, S. Altmannshofer, B. Weber, *Eur. J. Inorg. Chem.* **2011**, 2803–2818.
[28] B. Weber, R. Tandon, D. Himsl, *Z. Anorg. Allg. Chem.* **2007**, *633*, 1159–1162.
[29] a) P. Champagne, J. Desroches, J.-F. Paquin, *Synthesis* **2015**, *47*, 306–322; b) R. Berger, G. Resnati, P. Metrangolo, E. Weber, J. Hulliger, *Chem. Soc. Rev.* **2011**, *40*, 3496–3508.
[30] K. Dankhoff, C. Lochenie, F. Puchtler, B. Weber, *Eur. J. Inorg. Chem.* **2016**, *2016*, 2136–2143.
[31] W. Bauer, *Dissertation*, Ludwig-Maximilians-Universität München, München **2011**.
[32] A. Altomare, M. C. Burla, M. Camalli, G. L. Cascarano, C. Giacovazzo, A. Guagliardi, A. G. G. Moliterni, G. Polidori, R. Spagna, *J. Appl. Crystallogr.* **1999**, *32*, 115–119.
[33] a) G. Sheldrick, *SHELXL-97*, University of Göttingen, Göttingen, Germany **1997**; b) G. Sheldrick, *Acta Crystallogr., Sect. A* **2008**, *64*, 112–122.
[34] a) C. K. Johnson, M. N. Burnett, *ORTEP-III*, Oak-Ridge National Laboratory, Oak-Ridge, TN **1996**; b) L. Farrugia, *J. Appl. Crystallogr.* **1997**, *30*, 565.
[35] C. F. Macrae, P. R. Edgington, P. McCabe, E. Pidcock, G. P. Shilds, R. Taylor, M. Towler, J. van de Streek, C. F. Macrae, P. R. Edgington et al., *J. Appl. Crystallogr.* **2006**, *39*, 453–457.
[36] K. Lagarec, D. G. Rancourt, *Recoil*, Mössbauer Spectral Analysis Software for Windows 1.0, Department of Physics, University of Ottawa, Canada **1998**.

Received: December 23, 2019
Published Online: March 26, 2020

